1st Croatian Conference on Earthquake Engineering
1CroCEE
22-24 March 2021 Zagreb, Croatia

DOI: https://doi.org/10.5592/CO/1CroCEE.2021.91

The role of the soil heterogeneity in the seismic response of tunnel-soil systems

Glenda Abate[1], Sebastiano Corsico[2], Maria Rossella Massimino[3]

[1] *Assistant Researcher*, University of Catania, *glenda.abate@dica.unict.it*

[2] *PhD Student*, University of Catania, *sebastiano.corsico@unict.it*

[3] *Associate Professor*, University of Catania, *mmassimi@dica.unict.it*

Abstract

Nowadays, underground structures play a crucial role in transportation and utility networks in urban areas. Their static design has achieved a high level of accuracy. Instead, tunnels' efficient seismic design is not yet completely gotten, even due to the complex soil-tunnel interaction phenomena that occur during an earthquake. So, the few code regulations and guidelines about the seismic design of tunnels and the numerous parameters that affect the soil-tunnel systems' dynamic response have led the geotechnical research community to devote great attention to the study of the tunnel response under ground shaking. But, usually, dynamic analyses of coupled soil-tunnel systems are performed considering homogeneous soil at the tunnel's depth. Analytical solutions do not take specifically into account the possible heterogeneity of the soil crossed by the tunnel. To take into account this heterogeneity is necessary to move towards numerical approaches. The present paper investigates the role of soil heterogeneity and soil-tunnel interface conditions on tunnel seismic behaviour. Different numerical FEM parametric analyses were carried out, considering great differences in soil stiffness at the tunnel's depth. In particular, starting from a real case-history regarding the Catania (Italy) underground network, a cross-section characterized by a strong heterogeneity in terms of soil stiffness was firstly analysed. Then, the degree of heterogeneity was varied; furthermore, the soil-tunnel interface conditions were modified to comprise a large number of case studies. The achieved results were reported in terms of tunnel seismic bending moments and axial forces. The numerical results were also compared with those obtained using the closed-form solutions proposed by Wang (1993) and Penzien (2000) for homogeneous soil deposits.

Key words: soil dynamic characterization, FEM modelling, parametric analyses, soil-tunnel interface, bending moments, axial forces

1 Introduction

Today crucial role in transportation and utility networks of underground structures makes their vulnerability to seismic inputs a fundamental topic in earthquake engineering.

The few code regulations and guidelines about the seismic design of tunnels (e.g., [1] and [2]) and the numerous parameters that affect the dynamic response of the soil-tunnel systems have led the geotechnical research community to devote great attention to the study of the tunnel response under ground shaking. Several methods are available in the literature to evaluate the seismic response of underground structures [3; 10]. The results of these methods may significantly deviate, even under the same design assumptions, due to both inherent epistemic uncertainties and knowledge shortfall regarding some crucial issues that considerably affect the seismic response [11; 13]. About that, no analytical solution takes specifically into account the heterogeneity of the soil crossed by the tunnel. Usually, dynamic analyses of coupled soil-tunnel systems are performed considering homogeneous soil at the tunnel's depth.

So, the present paper shows a numerical parametric study conducted by a FEM code, assuming different soil configurations, to investigate the effects of the soil heterogeneity and soil-tunnel interface conditions on the tunnel seismic response. Starting from the underground network case-history of Catania (Italy) regarding a cross-section characterized by great soil heterogeneity, different soil impedance ratio values were adopted for the two soil layers crossed by the tunnel. Moreover, the soil-tunnel interface conditions were modified.

The response of the examined cases was discussed in terms of lining internal forces. These quantities were also evaluated by the closed-form solutions proposed by Wang [3] and Penzien [14], commonly used in the preliminary design stages of tunnels but developed for homogeneous soil crossed by the tunnel. The analytical and numerical results were compared to assess the validity and limitations of the analytical solutions.

2 The investigated tunnel-soil system

A cross-section of the underground network in Catania (Italy) was initially analysed [15; 18]; it belongs to the segment between the stations of Nesima and Misterbianco, next to Si3 borehole (Fig. 1).

The tunnel has a diameter equal to 10 m; it is 17 m below the ground surface (its axis is 22 m below the ground surface). The tunnelling was executed by a Tunnel Boring Machine. The final tunnel lining consists of a precast reinforced concrete ring (Young's modulus E_l = 36283 MPa, Poisson's ratio ν_l = 0.2, and damping ratio D_l = 5 %); each ring consists of 7 segments installed by an appropriate erector inside the TBM. Fig. 2.a shows the VS profile achieved by HVSR tests carried out during the geotechnical investigations performed in 2004 during the preliminary design of the underground line and in 2015 for the executive design. Unfortunately, the investigation survey concerned up to the depth of about 30 m, due to the instrumentations utilised in the performed HVSR tests. The shear waves velocity measured for this depth was equal to 345 m/s, which is very far from 800 m/s, the minimum value of *Vs* for the bedrock according to the Italian technical regulations [19] and the European Code 8 [20]. So, the *Vs* profile reported in Fig. 2.a as red line was supposed, neglecting the rock layer at z = 5-20 m, to find the depth at which V_s = 800 m/s (conventional bedrock). It was found at 80 m from the ground surface. This large assumption was unavoidable, due to the instrumentation utilised. No specific dynamic laboratory tests were performed for the geological formations at Si3 borehole. Thus, the typical $G(\gamma)$ and $D(\gamma)$ curves for Catania volcanic soil obtained by [21] were used (Fig. 2.b) to take into account the soil nonlinearity. For the very stiff soil (layer 1 in Fig. 2.a) $G(\gamma) = G_0$ and $D(\gamma) = D_0$ were used.

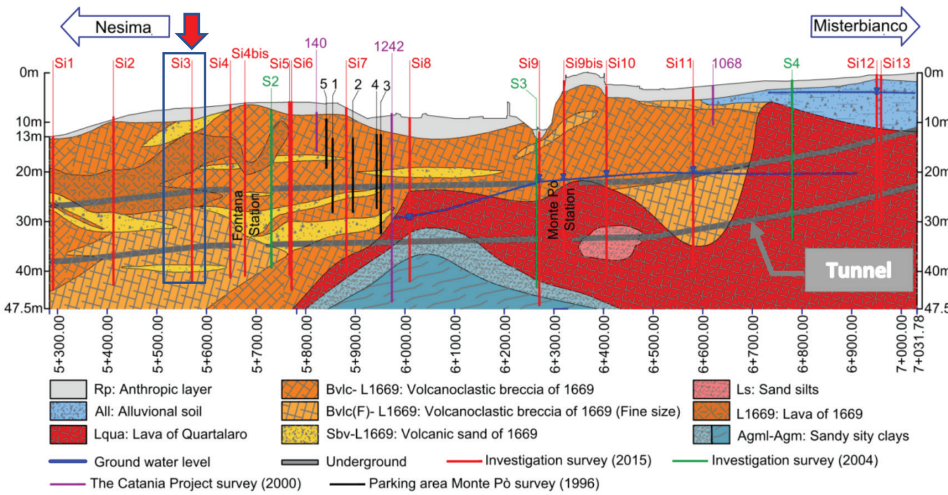

Figure 1. Soil profile and positions of the boreholes along the Nesima-Misterbianco segment of Catania underground

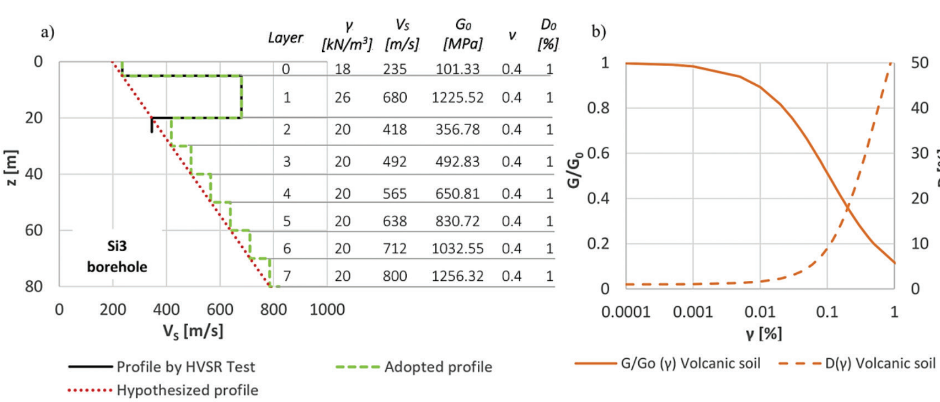

Layer	γ [kN/m³]	Vs [m/s]	Go [MPa]	ν	Do [%]
0	18	235	101.33	0.4	1
1	26	680	1225.52	0.4	1
2	20	418	356.78	0.4	1
3	20	492	492.83	0.4	1
4	20	565	650.81	0.4	1
5	20	638	830.72	0.4	1
6	20	712	1032.55	0.4	1
7	20	800	1256.32	0.4	1

Figure 2. a) Shear wave velocity profiles; b) $G(\gamma)$ and $D(\gamma)$ curves used for the equivalent linear analyses

3 FEM modelling

In order to evaluate the seismic response of the tunnel-soil system described in Section 2, a finite element modelling by using the ADINA code [22; 23], widely used in dynamic analyses [24; 27], was performed.
The 2D FEM model (Fig. 3) consisted of a stratified soil 80 m deep (up to the conventional bedrock) and 300 m wide (about 4 times the depth of the soil) to reduce the boundary effects. The FEM model was in plane strain conditions, and it was divided into 8 horizontal layers, according to the soil profile (green line) shown in Fig. 2.a. As regards the boundary conditions, the nodes of the soil vertical boundaries were linked by "constraint equations" that imposed the same horizontal and vertical displacements at the same depths [28], reproducing free-field conditions. The nodes at the base of the model were constrained only in the vertical direction; dashpots were implemented in the horizontal direction, to simulate the elastic bedrock according to [29]. The input motion was applied through the above dashpots as acceleration time history. It was a synthetic accelerogram scaled to PHA = 0.383g, which is the average expected value at the bedrock in Catania, for the Italian technical regulations [19] (considering the ultimate limit state associated with collapse or with other forms of structural failure which might endanger the safety of people: P_{VR} = 10 %; T_R = 1900 years). This accelerogram was obtained using a source mechanism modelling, assuming the source to be under the sea along the Hyblean-Maltese fault, according to the 1693 scenario earthquake for the city of Catania [30; 31].
A linear-equivalent-visco-elastic constitutive model was used for the soil to take into account its nonlinearity. The shear strain levels were evaluated by several 1D equivalent linear site response analyses, using the STRATA Code [32]. So, based on the $G(\gamma)$ and $D(\gamma)$ curves shown in Fig. 2.b, the updated values of G and D were estimated for each soil layer, except for the layer 1: it is a very stiff soil, so $G(\gamma) = G_0$ and $D(\gamma) = D_0$ were used. The achieved values of $G(\gamma)$ were in the range 0.60-0.90; instead, $D(\gamma)$ was achieved equal to about 4 %. The tunnel was modelled by a linear visco-elastic constitutive model, according to the previously described properties.
The damping matrix [C] was defined as a combination of the mass [M] matrix and the stiffness [K] matrix, according to the Rayleigh damping method. For the calibration of the Rayleigh damping coefficients a and b, the double frequency approach was used [33]:

$$\alpha = 2 \cdot \frac{D \cdot \omega_i \cdot \omega_j}{\omega_i + \omega_j}; \quad \beta = 2 \cdot \frac{D}{\omega_i + \omega_j} \tag{1}$$

in which $\omega_i = \omega_1 = (V_{s,av}/4H) \cdot 2\pi$ is the frequency of the soil at the first natural mode and $\omega_j = (2n-1) \cdot \omega_1$ is the frequency at the third relevant mode. According to [33], for soil columns with a thickness greater than 50 m, it is advisable to take into account the contributions of the higher modes. In the present case the Authors assumed n = 3 to obtain the damping within a constant period range.

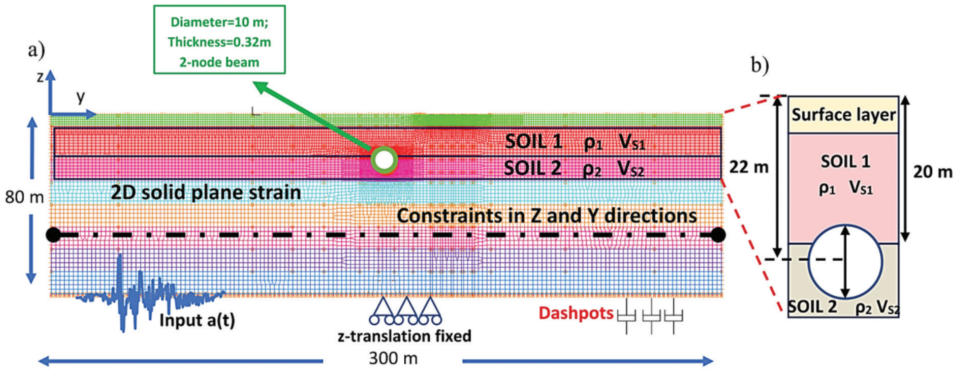

Figure 3. a) FEM model; b) zoom of the soil layers at the depth of the tunnel

4. The parametric analyses

Usually, dynamic analyses of coupled soil-tunnel systems are performed considering homogeneous soil at the tunnel's depth [34]. The present work deals with numerous parametric analyses carried out considering great differences of soil stiffness at the tunnel's depth (Fig. 3), using different values of the impedance ratio, *I*, according to the following expression:

$$I = \frac{\left(\rho_1 \cdot V_{S1}\right)}{\left(\rho_2 \cdot V_{S2}\right)} \tag{2}$$

where ρ_1 and V_{S1} are the density and shear wave velocity of the soil interacting with the upper part of the tunnel, while ρ_2 and V_{S2} are the density and shear wave velocity of the soil interacting with the bottom part of the tunnel (Fig. 3). So, in order to perform parametric analyses, the geotechnical parameters of the second and third layer were modified to obtain different values of *I* (Table 2). Initially, four values of *I* were used, performing four different models (Models 1-4). In particular, Model 3, characterized by I = 2.6, represented the real condition at the borehole Si3.

Per each impedance ratio (i.e., for each of the four models), three different tunnel-soil interface conditions were used: a) full-slip condition; b) no-slip condition; c) sliding contact with a friction coeffcient μ = 0.5.

Table 1. Main equivalent soil parameters for the two soil layers crossed by the tunnel for all the 10 developed FEM models

	Depth [m]	ρ [kg/m³]	$\mathbf{V_s}$ [m/s]	ρ [kg/m³]	$\mathbf{V_s}$ [m/s]
		Model 1: *I* = 1.0		**Model 2: *I* = 2.0**	
Soil 1	5÷20	2038	323	2650	496
Soil 2	20÷30	2038	323	2038	323
		Model 3: *I* = 2.6		**Model 4: *I* = 3.5**	
Soil 1	5÷20	2650	647	2650	647
Soil 2	20÷30	2038	323	2038	240
		Model 5: *I* = 1.5		**Model 6: *I* = 1.5**	
Soil 1	5÷20	2650	647	2650	647
Soil 2	20÷30	2038	560	2650	431
		Model 7: *I* = 3.0		**Model 8: *I* = 0.5**	
Soil 1	5÷20	2650	647	2038	323
Soil 2	20÷30	2038	280	2650	496
		Model 9: *I* = 0.3		**Model 10: *I* = 4.0**	
Soil 1	5÷20	2038	240	2650	647
Soil 2	20÷30	2650	647	2038	210

In a second phase, other values of *I* were considered (in the range 0.3 - 4.0), so totally ten FEM models were analysed (Table 2). Just the no-slip tunnel-soil interface condition was modelled for these added models (Models 5-10).

5 Results

Fig. 4 shows the numerical seismic bending moments *M* and axial forces *N* computed along the tunnel for the first four Models 1-4 considering all the tunnel-soil interface conditions previously explained. Two different coloured bands highlight the two different layers (1 and 2) crossed by the tunnel.

The strong influence of the heterogeneity of the soil crossed by the tunnel was found in *M* distribution. For higher values of *I* (from Model 1 to Model 4), higher values of *M* were evaluated, achieving a strongly non-uniform bending moment distribution along the tunnel: very small *M* at the depth of Soil 1 (stiff soil); higher values at the depth of Soil 2 (soft soil); and above all important peaks at the soil stiffness discontinuity. As expected, the best distribution of the bending moments was observed for Model 1, representing the homogeneous soil condition at the tunnel depths (*I* = 1.0). As for the three different tunnel-soil interface conditions, very similar results to each other were achieved.

Unlike the bending moments, the obtained axial forces did not vary much with *I*. Regarding the three different soil-tunnel interface conditions, higher values of *N* were achieved in the no-slip condition, due to the higher concentration of stress along the tunnel,

generated by the lack of relative sliding between soil and tunnel. For the partial-slip condition, lower values of around 20 % were achieved. Finally, for the full-slip condition constant low values were achieved.
So, it is advisable to carefully evaluate bending moment distributions for tunnel crossing heterogeneous soil and to require the necessary geotechnical in-situ tests for exactly estimating the depth of the soil stiffness discontinuity and the impedance ratio I. Moreover, the achieved numerical results suggested the use of the no-slip tunnel-soil interface condition in numerical modelling to guarantee the highest possible safety condition. Consequently, just the no-slip soil-tunnel interface condition was adopted for Models 5-10, as previously introduced.
Fig. 5.a and Fig. 5.b show the comparison between the analytical internal forces and the numerical ones for all the ten developed models (represented by ten different indicators). Similarly, Fig. 5.c and 5.d reports the maxima internal forces versus the soil impedance ratios. Analytical internal forces were computed according to the solutions developed by Wang [3] and Penzien [14], which, as previously written, were developed only for tunnels in homogeneous soil. However, the Authors fit them for the heterogeneous profile of the soil crossed by the tunnel, adopting two different values of V_S for the two layers surrounding the tunnel; the first value V_{S1} was used for 23° < θ< 157° ("Soil 1" in Fig. 3.b); the second value V_{S2} was used for 0° < θ< 23° and 157° < θ< 360° ("Soil 2" in Fig. 3.b). Moreover, also two different average values of soil shear strains were evaluated for the two above-mentioned layers.
Regarding the bending moments, a good agreement between numerical and analytical results was achieved, even if it became less satisfactory for strong heterogeneity (I = 0.3, 3.0, 3.5 and 4.0). As for the dynamic axial forces, the Penzien solution [14] furnished very low values in comparison with the numerical ones; the Wang solution [3] furnished very high values in comparison with the numerical ones only for Models 3, 4, 7, 10, i.e., for I > 2.5. The increasing of the impedance ratio I led to an increasing of the gap between analytical and numerical results.
As for the M_{max} vs I trend, it is possible to observe that M strongly depended on I and the minimum values were reached for values of I next to 1; on the other hand, the further I was away from 1, the higher the value of M. As for N_{max} vs I trends, it is possible to observe that the numerical axial forces did not significantly vary with I; instead, they strongly increased with I according to the Wang approach [3], due to the increasing of the shear strain increasing with I. Finally, Penzien approach [14] gave very low values, as observed by other researchers [34].

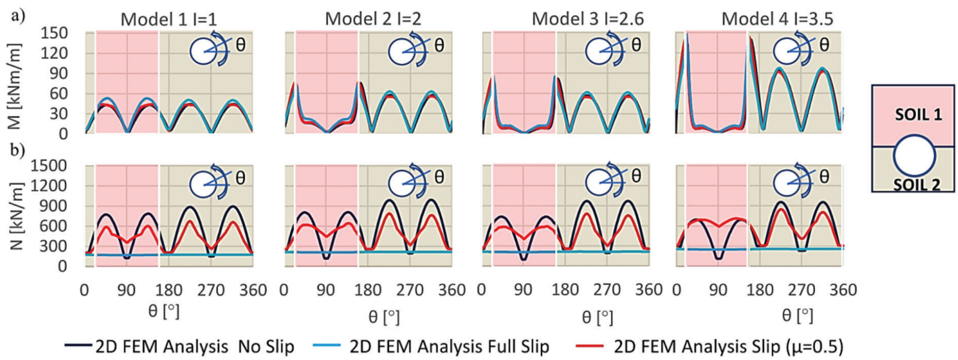

Figure 4. a) Numerical dynamic bending moments and b) numerical dynamic axial forces for the first four analysed models

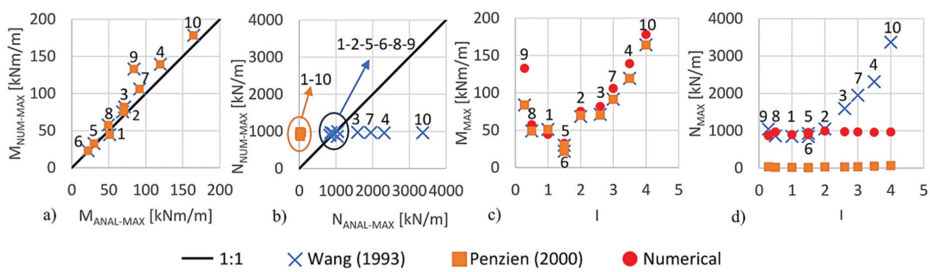

Figure 5. Comparison between numerical and analytical results for all the 10 FEM models: a) numerical bending moments versus analytical bending moments; b) numerical axial forces versus analytical axial forces; c) Mmax versus I; d) Nmax versus I

6 Conclusions

The paper deals with the effect of soil heterogeneity on seismic tunnel response. Different numerical FEM analyses were carried out, considering significant differences in the soil layers' stiffness crossed by a tunnel. The soil impedance ratio *I*, evaluated as the ratio between the density and shear waves velocity of the soil interacting with the upper part of the tunnel and the density and shear waves velocity of the soil interacting with the bottom part of the tunnel, was varied. The numerical results were also compared with the closed-form solutions by Wang and Penzien, developed for homogeneous soil deposits. These closed-form solutions were here used considering different shear strains for the different soil layers to adapt these solutions to non-homogeneous soil deposits.

The strong influence of the heterogeneity of the soil crossed by the tunnel on the tunnel seismic bending moment *M* distribution was found. A strange bending moment distribution along the tunnel was achieved for high values of *I*, with important peaks at the soil stiffness discontinuity. As expected, the best distribution of the bending moments

was observed for I = 1.0 (homogeneous soil). As for the three different tunnel-soil interface conditions (no-slip, full-slip, partial slip), very similar results to each other were achieved. Regarding the seismic axial forces in the tunnel, the numerical values did not vary much with I. Regarding the three different soil-tunnel interface conditions, higher N values were achieved for the no-slip condition. So, this condition is preferable in numerical modelling to guarantee the highest possible safety.
As for the comparison with the analytical results, a good agreement in terms of M was achieved only taking into account different shear strains for the different soil layers, even if it is less satisfactory for strong heterogeneity. Regarding N, Penzien solution furnished very low values; Wang solution provided very high values compared to the numerical ones only for $I > 2.5$. The increasing of the impedance ratio, I, led to an increasing gap between analytical and numerical results.
The results revealed the need to increase numerical analyses to estimate lining forces more consistent with the soil-tunnel system's real behaviour. The future goal is developing easy-to-use analytical solutions that will take into account the heterogeneity of the soil crossed by a tunnel.

Acknowledgements

Financial supports provided by the DPC/ReLUIS 2018 (AQ DPC/ReLUIS 2014-2018) Research Project, which has been funded by the Italian Civil Protection Department, and by the "Transport Infrastructure Management in Urban Contest" Interdepartmental Project allowed the authors to achieve the results reported in this paper.

References

[1] ISO 23469 (2005): Bases for design of structures - Seismic actions for designing geotechnical works, International Organisation for Standardisation.

[2] AFPS/AFTES (2001): Guidelines on earthquake design and protection of underground structures, Working group of the French association for seismic engineering (AFPS) and French Tunnelling Association (AFTES) Version 1.

[3] Wang, J.-N. (1993): Seismic Design of Tunnels: A State-of-the-Art Approach, Monograph, monograph 7. Parsons, Brinckerhoff, Quade and Douglas Inc, New York.

[4] Power, M., Rosidi, D., Kaneshiro, J., Gilstrap, S., Chiou, S.J. (1998): Summary and evaluation of procedures for the seismic design of tunnels. Final Report for Task 112-d-5.3(c). National Centre for Earthquake Engineering Research, Buffalo, New York.

[5] Hashash, Y.M.A., Hook, J.J., Schmidt, B. and Yao, J.I-C. (2001): Seismic design and analysis of underground structures, Tunnelling and Underground Space Technology, 16 (2), 247-293.

[6] Wang, W.L., Wang, T.T., Su, J.J., Lin, C.H., Seng, C.R., Huang, T.H. (2001): Assessment of damage in mountain tunnels due to the Taiwan Chi-Chi earthquake. Tunnelling and Underground Space Technology, 16, 133–150.

[7] Hashash, Y.M.A., Park, D., Yao, J.I.C. (2005): Ovaling deformations of circular tunnels under seismic loading, an update on seismic design and analysis of underground structures, Tunneling and Underground Space Technology 20, 435–441.

[8] Kontoe, S., Zdravkovic, L., Potts, D., Mentiki, C. (2008): Case study on seismic tunnel response. Canadian Geotechnical Journal, 45, 1743–1764.

[9] Wang, Z.Z., Gao, B., Jiang, Y.J., Yuan, S. (2009): Investigation and assessment on mountain tunnels and geotechnical damage after the Wenchuan earthquake. Science China Technological Sciences, 52(2), 549–558.

[10] FHWA (2009): Technical manual for design and construction of road tunnels – Civil elements, U.S. Department of transportation, Federal Highway Administration, Publication No. FHWA-NHI-09-010, March 2009.

[11] Anastasopoulos I, Gerolymos N., Drosos V, Kourkoulis R, Georgarakos T, Gazetas G (2007). Nonlinear Response of Deep Immersed Tunnel to Strong Seismic Shaking. Journal Geotechnical Geoenvironmental Engineering, 133 (9), 1067-1090.

[12] Gazetas, G. (2014): Case histories of tunnel failures during earthquakes and during construction, Proc. of the Half-Day Conference, A Tunnel/Underground Station Failure Conference, by the Israeli Geotechnical Society, 19th of January 2014.

[13] Pitilakis, K., Tsinidis, G. (2014): Performance and seismic design of underground structures, Earthquake geotechnical engineering design, Chapter 11, 279-340, Springer international publishing, Editors: Michele Maugeri, Claudio Soccodato.

[14] Penzien, J. (2000): Seismically-induced racking of tunnel linings, Earthquake Engineering and Structural Dynamics, 29, 683-691.

[15] Abate, G., Corsico, S., Massimino, M.R. (2016): FEM Modelling of the Seismic Behaviour of a Tunnel-soil-Aboveground Building System: A Case History in Catania (Italy). Procedia Engineering, 158 (2016), 380-385. ISSN: 1877-7058. https://doi.org/10.1016/j.proeng.2016.08.459.

[16] Abate, G., Massimino, M.R. (2017a): Numerical modelling of the seismic response of a tunnel–soil–aboveground building system in Catania (Italy). Bulletin of Earthquake Engineering 15 (1), 469-491.

[17] Abate, G., Massimino, M.R. (2017b): Parametric analysis of the seismic response of coupled tunnel–soil–aboveground building systems by numerical modelling. Bulletin of Earthquake Engineering 15 (1), 443-467.

[18] Abate, G., Grasso, S., Massimino, M.R. (2019): The role of shear wave velocity and non-linearity of soil in the seismic response of a coupled tunnel-soil-above ground building system. Geosciences (Switzerland), 9 (11), 473.

[19] NTC 2018: D.M. 17/01/18 - Updating of technical standards for buildings, Official Journal of the Italian. 17th January 2018 (in Italian).

[20] EC8 (2003): Design of structures for earthquake resistance. European Pre-standard. ENV 1998. Europ. Com. for Standard. Bruxelles.

[21] Maugeri, M., Cavallaro, A., Grasso, S. (2006): Volcanic soil characterisation and site response analysis in the city of Catania, Proc. of the 8th National Conference on Earthquake Engineering, San Francisco, CA, United States; April 18-22, 2006.

[22] Bathe KJ (1996): Finite Element Procedures, Prentice Hall, Engineering Cliffs, N Journal.

[23] ADINA (2008): Automatic Dynamic Incremental Nonlinear Analysis. Theory and Modelling Guide, ADINA R&D, Inc. Watertown, USA.

[24] Grassi, F., Massimino, M.R. (2009): Evaluation of kinematic bending moments in a pile foundation using the finite element approach. WIT Transactions on the Built Environment, 104, 479-488.

[25] Kirtas, E., Rovithis, E., Pitilakis, K. (2009): Subsoil Interventions Effect on Structural Seismic Response. Part I: Validation of Numerical Simulations. Journal of Earthquake Engineering, 13, 155–169.

[26] Abate, G., Massimino, M.R., Maugeri, M. (2015): Numerical Modelling of centrifuge tests on tunnel-soil systems. Bulletin of Earthquake Engineering, 13 (7), 1927-1951.

[27] Maugeri, M., Abate, G., Massimino, M.R. (2012): Soil-Structure Interaction for Seismic Improvement of Noto Cathedral (Italy). Geotechnical, Geological and Earthquake Engineering, 16, 217-239.

[28] Abate, G., Massimino, M.R. (2016): Dynamic soil-structure interaction analysis by experimental and numerical modelling. Rivista Italiana di Geotecnica, 50 (2), 44-70.

[29] Lysmer, J., Kuhlemeyer, R.L. (1969): Finite dynamic model for infinite media. Journal of the Engineering Mechanics Division, ASCE, 95 (4), 859-878.

[30] Azzaro, R., Barbano, M.S., Moroni, A., Mucciarelli, M., Stucchi, M. (1999): The Seismic History of Catania, Journal of Seismology, 3 (3), 235-252.

[31] Azzaro, R., Barbano, M. S. (2000): Seismogenetic Features of SE Sicily and Scenario Earthquakes for Catania. The Catania Project: Earthquake Damage Scenarios for a High-Risk Area in the Mediterranean, part I: Seismotectonic Framework and Earthquake Scenarios, CNR-Gruppo Nazionale per la Difesa dai Terremoti, Roma, 9-13.

[32] Kottke, A.R., Rathje, E.M. (2008): Technical Manual for STRATA. PEER Report 2008/10. University of California, Berkeley, California.

[33] Hashash, Y.M.A., Park, D. (2002): Viscous damping formulation and high frequency motion propagation in non-linear site response analysis, Soil Dynamics and Earthquake Engineering, 22 (7), 611-624.

[34] Argyroudis, S., Tsinidis, G., Gatti, F., Pitilakis, K. (2017): Effects of SSI and lining corrosion on the seismic vulnerability of shallow circular tunnels. Soil Dynamics and Earthquake Engineering, 98, 244-256. https://doi.org/10.1016/j.soildyn.2017.04.016.